



The molecular mass of dextran used to modify magnetite nanoparticles affects insulin amyloid aggregation



Katarina Siposova^a, Kristyna Pospiskova^b, Zuzana Bednarikova^{a,c}, Ivo Safarik^{b,d},
Mirka Safarikova^d, Martina Kubovcikova^e, Peter Kopcansky^e, Zuzana Gazova^{a,*}

^a Department of Biophysics, Institute of Experimental Physics, Slovak Academy of Sciences, Kosice, Slovakia

^b Regional Centre of Advanced Technologies and Materials, Palacky University, Olomouc, Czech Republic

^c Department of Biochemistry, Faculty of Science, Safarik University, Kosice, Slovakia

^d Department of Nanobiotechnology, Biology Centre, ISB, CAS, Ceske Budejovice, Czech Republic

^e Department of Magnetism, Institute of Experimental Physics, Slovak Academy of Sciences, Kosice, Slovakia

ARTICLE INFO

Keywords:

Amyloid aggregation
Nanoparticles
Magnetic fluid
Dextran
Insulin
Anti-amyloid activity
Amyloid fibrils

ABSTRACT

Protein transformation from its soluble state into amyloid aggregates is associated with amyloid-related diseases. Amyloid deposits of insulin fibrils have been found in the sites of subcutaneous insulin application in patients with prolonged diabetes. Using atomic force microscopy and ThT fluorescence assay we have investigated the interference of insulin amyloid aggregation with superparamagnetic Fe₃O₄-based nanoparticles (SPIONs) coated with dextran (DEX); molecular mass of dextran was equal to 15–20, 40 or 70 kDa. The obtained data indicate that all three types of dextran coated nanoparticles (NP-FeDEXs) are able to inhibit insulin fibrillization and to destroy amyloid fibrils. The extent of anti-amyloid activities depends on the properties of NP-FeDEXs, mainly on the size of nanoparticles which is determined by molecular mass of dextran molecules. The most effective inhibiting activity was observed for the smallest nanoparticles coated with 15–20 kDa dextran. Contrary, the highest destroying activity was observed for the largest NP-FeDEX (70 kDa dextran).

1. Introduction

More than twenty human proteins can fold abnormally to form pathological amyloid aggregates that are associated with a number of diseases including Alzheimer's disease, type II diabetes, Parkinson's and Creutzfeldt-Jacob's diseases [1]. The common feature of amyloid diseases is the presence of amyloid deposits mainly consisting of aggregated poly/peptide typical for given disease. The formation of amyloid aggregates is described by a nucleation-growth process [2]. It was observed that many proteins can form amyloid structures with characteristic cross-β stacking perpendicular to the long axis of the fiber [3–5].

Insulin is a small protein hormone that is crucial for control of the glucose metabolism and diabetes treatment. Insulin belongs to the group of globular proteins which amyloid deposits have been found in the sites of subcutaneous drug application in patients with prolonged diabetes treatment [6]. Insulin amyloid aggregation causes also a serious problem in the production, storage and delivery of this important biopharmaceutical compound as well as in application of the insulin pumps.

Although a great efforts have been made to understand the pathogenesis of these diseases and design effective therapy there is still no treatment for amyloid-related diseases. Nevertheless, inhibition and/or reduction of amyloid aggregates have been considered as the primary therapeutic strategy [7,8]. For that purpose, a large number of amyloid aggregation inhibitors were contemplated as potential drug candidates. In recent years, many efforts have been focused on the investigation of the effect of nanoparticles on protein amyloid aggregation as they have unique properties such as the high surface/volume ratio, size, surface charge, composition and biocompatibility. It was found that NPs affect amyloid aggregation differently; they can enhance the rate of amyloid fibrillization [9–11], as well as significantly reduce formation of amyloid fibrils [12–16,17].

Ferromagnetic iron cannot be used directly in biological applications due to their high reactivity in aqueous environments. For biomedical applications coated nanoparticles (core-shell-structured nanoparticles) are used instead of bare nanoparticles because they are less toxic, have greater dispersibility, better conjugation with other bioactive molecules and increased chemical and thermal stability [18]. The potential use of superparamagnetic iron oxide nanoparticles

* Correspondence to: Institute of Experimental Physics, Slovak Academy of Sciences, Watsonova 47, 043 53 Kosice, Slovakia.
E-mail address: gazova@saske.sk (Z. Gazova).

(SPION) in biomedical applications arise from their small size, their superparamagnetic properties, and their generally good biocompatibility. There are only few reports on the interaction of the SPIONs with amyloidogenic proteins. Mahmoudi *et al.* investigated effect of magnetic nanoparticles on kinetic of A β fibrillization [19]. Interestingly, lower concentrations of SPIONs caused inhibition of fibrillization, the higher concentrations enhance the rate of fibril formation.

We studied the interference of Fe₃O₄-based dextran coated nanoparticles (NP-FeDEXs) with insulin amyloid aggregation using Thioflavin T fluorescence assay and atomic force microscopy. For this study three types of dextran, which differ in molecular mass (Mw=15 – 20 kDa, 40 kDa and 70 kDa), were used to improve the biocompatibility of magnetite nanoparticles. It was found that molecular mass of dextran used for nanoparticle coating determines the size and anti-amyloid activities of NP-FeDEXs.

2. Materials and methods

2.1. Materials

Human recombinant insulin (expressed in yeast, lot number I2643, ~24 IU/mg protein), Thioflavin T (ThT) and dextran from *Leuconostoc* spp. with different molecular mass (15–20 kDa, 40 kDa and 70 kDa) were obtained from Sigma Chemical Company (St. Louis, MO). All other chemicals were of analytical grade and purchased from Sigma or Fluka.

2.2. Preparation of magnetic nanoparticles

Dextran stabilized magnetic nanoparticles consisting of Fe₃O₄ (magnetite) core (NP-FeDEX) were prepared using the slightly modified Molday procedure [20]. Briefly, 19 g of dextran was dissolved in 75 ml of water while 5 g of FeCl₃·6H₂O and 2.1 g of FeCl₂·4H₂O were dissolved in 13 ml of 2 M HCl. Both solutions were mixed together and put to water bath (60 °C). Then, under mixing, 75 ml of 7.5% ammonium hydroxide was added dropwise and the mixing continued for another 15 min at 60 °C. The next day the ferrofluid was centrifuged (5000 rpm, 45 min; Universal 320, Hettich Zentrifugen, Germany).

2.3. Dynamic light scattering

DLS evaluates the fluctuations of scattered light intensity diffracted from nanoparticles undergoing the steady Brownian motion in suspension. Hydrodynamic size of nanoparticles in ferrofluid samples was determined using Zetasizer Nano ZS (Malvern Instruments, UK). Samples were diluted and measured in disposable sizing cuvettes at 25 °C and 173° scattering angle. Zeta potential of the samples was obtained by the same instrument using electrophoretic light scattering and disposable capillary cell for sample measurement.

2.4. Amyloid fibrillization of insulin

Insulin was dissolved to a final concentration of 10 μ M in 50 mM phosphate buffer, pH 7.5. Spontaneous amyloid fibrillization of insulin was induced by incubation of the solution at 65 °C and constant stirring (1200 rpm) for 2 h. Formation of fibrils was monitored by Thioflavin T assay and atomic force microscopy.

2.5. Thioflavin (ThT) assay

ThT is a cationic benzothiazole dye showing enhanced fluorescence upon binding to protein amyloid fibrils. ThT was added to the insulin samples (10 μ M) to a final concentration of 20 μ M. Measurements were performed in a 96-well plate by a Synergy MX (BioTek) spectrofluorimeter after 60 min incubation. The excitation was set at 440 nm

and the emission recorded at 485 nm. The excitation and emission slits were adjusted to 9.0/9.0 nm and the top probe vertical offset was 6 mm. All ThT fluorescence experiments were performed in triplicate and the final value is the average of measured values.

2.6. AFM measurements

Samples for AFM were prepared by drop casting of solution on the surface of freshly cleaved mica and after 5 min adsorption they were rinsed with ultrapure water added dropwise. Then the sample was left to dry before scan. AFM images were taken by a Scanning Probe Microscope (Veeco di Innova, Bruker AXS Inc., Madison) in a tapping mode in ambient conditions, using uncoated silicon cantilevers NCHV (Bruker AFM Probes, Camarillo) with nominal resonance frequency 320 kHz and spring constant 42 N/m. No smoothing or noise reduction was applied.

2.7. Anti-amyloid activity of NP-FeDEX

ThT fluorescence assay was used to investigate the ability of studied nanoparticles (NP-FeDEXs) to inhibit insulin fibrillization as well as to destroy pre-formed insulin fibrils. For evaluation of the inhibiting activities the nanoparticles were added to 10 μ M (58 μ g ml⁻¹) insulin solution (50 mM phosphate buffer, pH 7.5) at concentrations ranging from 2.9 μ g ml⁻¹ to 1160 μ g ml⁻¹ (concentration of Fe₃O₄ magnetite core) and the mixtures were exposed to the conditions inducing amyloid aggregation as described in part 2.4. Destroying activities were measured after 24 h incubation of insulin amyloid fibrils (10 μ M) with nanoparticles at concentrations from 2.9 μ g.ml⁻¹ to 1160 μ g.ml⁻¹ (concentration of Fe₃O₄ magnetite core) at 37 °C. The values of fluorescence were normalized to the fluorescence determined for untreated amyloid fibrils (taken as 100%). Each experiment was performed in triplicates and values represent the average of the obtained values. As a control, the fluorescence of each NP-FeDEX on its own and in presence of ThT was measured. The IC₅₀ and DC₅₀ values (IC₅₀ - concentration of NP-FeDEX leading to 50% inhibition of insulin amyloid fibrillization; DC₅₀ - concentration of NP-FeDEX causing 50% destruction of insulin fibrils) were obtained by fitting the average values by a nonlinear least-squares method with the sigmoidal logistic 3 parameters equation ($y=a/[1+(x/x_0)^b]$).

3. Results and discussion

Superparamagnetic iron oxide nanoparticles (SPIONs) are of particular importance due to their high potential to be used as therapeutical agents. To increase their biocompatibility the Fe₃O₄ core is often coated by various agents such as proteins or polysaccharides. In our study we examined the interference of dextran coated magnetite nanoparticles (NP-FeDEXs) with insulin amyloid aggregation. Dextran used for coating had different molecular mass, namely 15–20 kDa (DEX_1), 40 kDa (DEX_2) and 70 kDa (DEX_3) in order to investigate the effect of the size of nanoparticles resulting from different coating layer size on the amyloid aggregation.

3.1. Physico-chemical properties of studied nanoparticles

The physico-chemical properties of studied nanoparticles were determined by dynamic light scattering and obtained nanoparticle characteristics, namely the hydrodynamic diameter (D_{HYD}), polydispersity index (PDI) and zeta potential (ZP) are given in Table 1. The nanoparticles have been visualized using the atomic force microscopy (AFM). All types of nanoparticles exhibited similar spherical morphology. The representative AFM image of nanoparticles coated with 15–20 kDa dextran (NP-FeDEX_1) is presented in Fig. 3E.

According to the data presented in Table 1 the average hydrodynamic diameter positively correlates with molecular mass of dextran

Table 1
Characteristics of NP-FeDEXs and their anti-amyloid abilities.

	M_w [kDa]	D_{HYD} [nm]	PDI	ZP [mV]	IC_{50} [$\mu\text{g}\cdot\text{ml}^{-1}$]	DC_{50} [$\mu\text{g}\cdot\text{ml}^{-1}$]
NP-FeDEX_1	15–20	76.9 ± 0.4	0.165	-12 ± 2.9	48.2 ± 2.7	74.4 ± 6.0
NP-FeDEX_2	40	90.5 ± 0.7	0.145	-8.32 ± 2.7	58.7 ± 3.5	68.1 ± 5.4
NP-FeDEX_3	70	124.3 ± 1.4	0.157	-8.68 ± 2.8	84.6 ± 3.9	50.9 ± 4.7

M_w - Molecular mass of dextran used for coating, D_{HYD} - Hydrodynamic diameter, PDI - Polydispersity index, ZP - Zeta potential determined from DLS.

used for coating of the magnetite nanoparticles. The smallest hydrodynamic diameter of about 77 nm was obtained for nanoparticles coated with 15–20 kDa dextran (NP-FeDEX_1). For 40 kDa dextran nanoparticles (NP-FeDEX_2) the hydrodynamic diameter is 90.5 nm and the largest diameter of 124.3 nm was determined for nanoparticles coated with 70 kDa dextran (NP-FeDEX_3). The values of polydispersity index are comparable for all three types of nanoparticles, varying from 0.145–0.165. It suggests the similar level of the component arrangement. Zeta potential of the dextran coated nanoparticles has negative values which vary according to the type of dextran. The NP-FeDEX_2 and NP-FeDEX_3 have similar values (-8.32 and -8.68 mV) which indicate the negative charges on the nanoparticles surface. A slightly greater value of -12 mV was observed for nanoparticles NP-FeDEX_1 coated with the lowest molecular weight dextran. These data suggest that stability of all three types of the NP-FeDEXs is comparable. From obtained results we assume that the significant difference due to various dextrans coating layer were detected for the size and zeta potential of nanoparticles.

3.2. Anti-amyloid activity of dextran coated nanoparticles

The inhibiting and destroying activities of all three types of NP-FeDEXs were studied in Fe_3O_4 concentrations range from $2.9 \mu\text{g}\cdot\text{ml}^{-1}$ to $1160 \mu\text{g}\cdot\text{ml}^{-1}$ at fixed protein concentration ($10 \mu\text{M} = 58 \mu\text{g}\cdot\text{ml}^{-1}$). The relative fluorescence intensities (normalized to the signal of amyloid aggregates alone) obtained in presence of all types of nanoparticles are shown in Fig. 1. It was found that all studied nanoparticles inhibit insulin fibrillization in a concentration-dependent manner and decrease of fluorescence intensities follows a sigmoidal decay (Fig. 1A). Destroying activities of nanoparticles over the same concentration range were also observed using Thioflavin T assay. The sigmoidal decay of fluorescence intensities after treatment of insulin fibrils with dextran nanoparticles are shown in Fig. 1B.

From the curves the concentrations of magnetite nanoparticles at 50% inhibiting (IC_{50}) and 50% destroying (DC_{50}) activities were

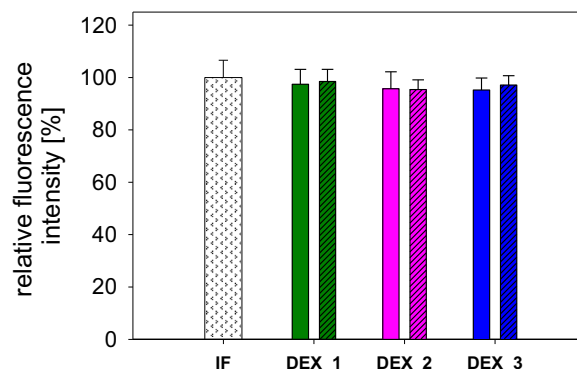


Fig. 2. Effect of dextrans DEX_1, DEX_2 and DEX_3 on insulin amyloid fibrillation (empty bars) and insulin fibrils (hatched bars) detected by ThT assay. The data were normalized to fluorescence intensity detected for untreated insulin fibrils (IF).

calculated and are presented in Table 1. The obtained data clearly show that NP-FeDEXs interfere with insulin amyloid aggregation at very low concentrations ($\mu\text{g}\cdot\text{ml}^{-1}$). Moreover, the IC_{50} and DC_{50} values have shown correlation with the molecular mass of dextran. In case of inhibition the most effective inhibition activity is observed for the smallest dextran-modified nanoparticles coated with 15–20 kDa dextran ($D_{HYD}=76.9$ nm, $IC_{50}=48.2 \mu\text{g}\cdot\text{ml}^{-1}$). Bigger nanoparticles coated with higher molecular mass dextrans (NP-FeDEX_2) have slightly higher IC_{50} values of $58.7 \mu\text{g}\cdot\text{ml}^{-1}$. The highest IC_{50} value was determined for NP-FeDEX_3 nanoparticles ($84.6 \mu\text{g}\cdot\text{ml}^{-1}$) which indicate less effective inhibition abilities.

The opposite dependence was observed for destroying activities of studied NP-FeDEXs. The highest ability to destroy insulin fibrils was detected for NP-FeDEX_3 ($DC_{50}=50.9 \mu\text{g}\cdot\text{ml}^{-1}$) characterized by the largest size ($D_{HYD}=124.3$ nm), while for smaller nanoparticles (NP-FeDEX_2 and NP-FeDEX_1) the gradual decline of destroying activities were observed with $DC_{50}=68.1 \mu\text{g}\cdot\text{ml}^{-1}$ and $74.4 \mu\text{g}\cdot\text{ml}^{-1}$, respectively.

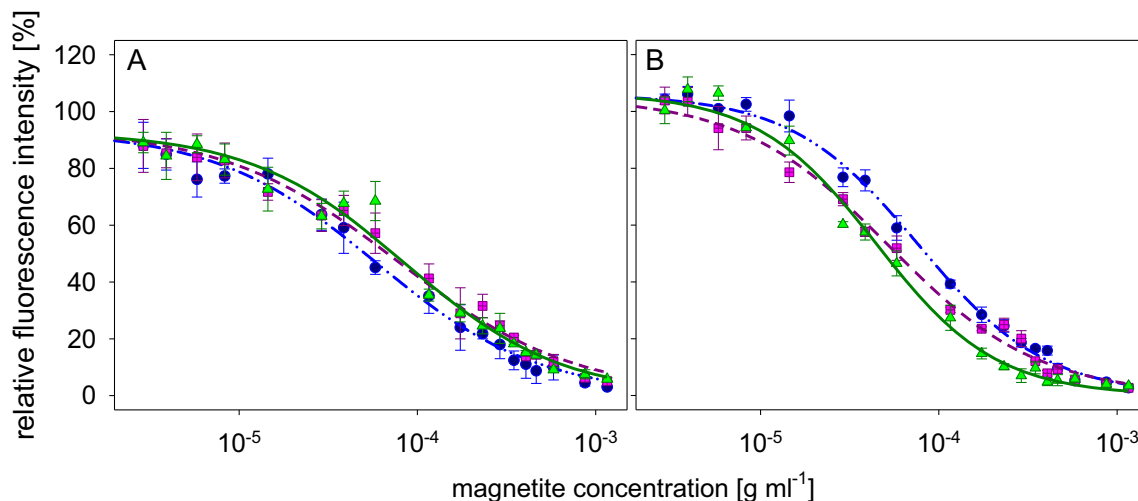


Fig. 1. The effect of NP-DEXs on insulin amyloid fibrillization (A) and insulin amyloid fibril degradation (B) monitored by ThT assay: NP-DEX_1 (triangles, solid line), NP-DEX_2 (squares, dashed line) and NP-DEX_3 (circles, dashed-dotted-dotted line).

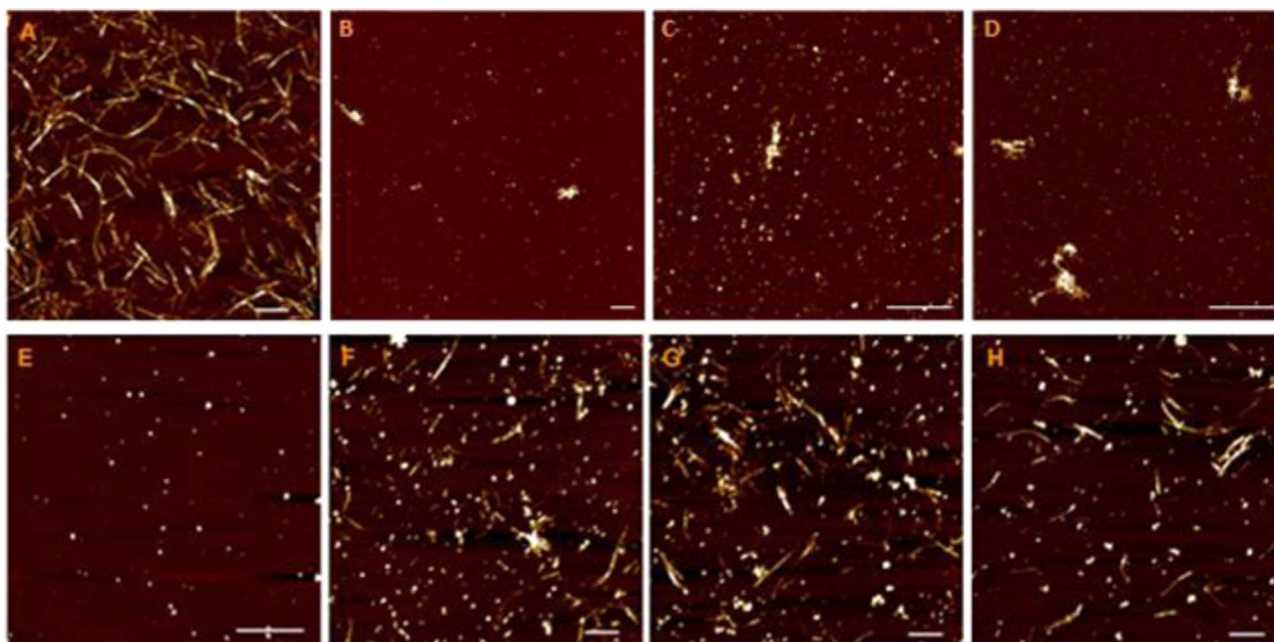


Fig. 3. AFM images of insulin amyloid fibrils (IF) formed in absence (A) and presence of NP-FeDEX_1 (B), NP-FeDEX_2 (C) and NP-FeDEX_3 (D) (ratio IF: NP-FeDEX=1:2). Destruction of insulin amyloid fibrils after 24 h incubation with NP-FeDEX_1 (F), NP-FeDEX_2 (G) and NP-FeDEX_3 (H). AFM image of NP-FeDEX_1 alone (E). Scale bars are 1 μm .

Next, we were interested whether dextran itself has the ability to affect insulin amyloid aggregation. We investigated inhibiting and destroying activities of dextrans used as coating agents at the concentration corresponding to the highest concentration of dextran used in experiments with NP-FeDEXs, namely at ratio protein: NP-FeDEX=1:20. The measured fluorescence intensities were comparable to the one detected for untreated insulin amyloid fibrils (IF) (Fig. 2). The obtained results indicate that dextran alone (all three types) has no significant ability to inhibit insulin amyloid fibrillization and to destroy the insulin amyloid fibrils.

Atomic force microscopy was used to verify results obtained using ThT assay and for direct visualization of formed amyloid aggregates before and after treatment with dextran nanoparticles. AFM image of insulin amyloid fibrils (Fig. 3A) shows typical amyloid morphology of aggregates displaying long fibrillar structure and protofibrillar twisting with tendency of lateral association. AFM images demonstrate that presence of all types of dextran coated nanoparticles caused significant inhibition of amyloid fibrillization as only a few very small amorphous-like aggregates were observed (Fig. 3B–D). The destroying activities of nanoparticles were examined after 24 h incubation of NP-FeDEXs with insulin amyloid fibrils. AFM images show that treatment of insulin amyloid fibrils with nanoparticles leads to their destruction and reduction of their amount (Fig. 3F–H). We observed the thinner and shorter fibrils as well as the aggregates with globular morphology. The results obtained by AFM strongly indicate that interference of NP-FeDEX with insulin amyloid aggregation leads to inhibition of insulin amyloid fibrillization and destruction of amyloid fibrils.

Using ThT fluorescence assay we have investigated in which phase of fibrillization the interaction between nanoparticles and insulin leads to inhibition of fibril formation. The growth curves of the insulin fibril formation in the absence and the presence of dextran-coated nanoparticles (w/w insulin: Fe_3O_4 ratio=1:2) are presented in Fig. 4. In the absence of the nanoparticles amyloid fibrillization of insulin follows a sigmoidal kinetics, whereby the characteristic lag phase (taking approx. 30 min) was followed by elongation step and fibril formation was completed after about 2 h (Fig. 4, crosses). The shape of insulin amyloid aggregation curve corresponds to representative nuclei-dependent growth curve of amyloid fibrillization. As expected, the presence of nanoparticles affected the kinetics of insulin fibrillization.

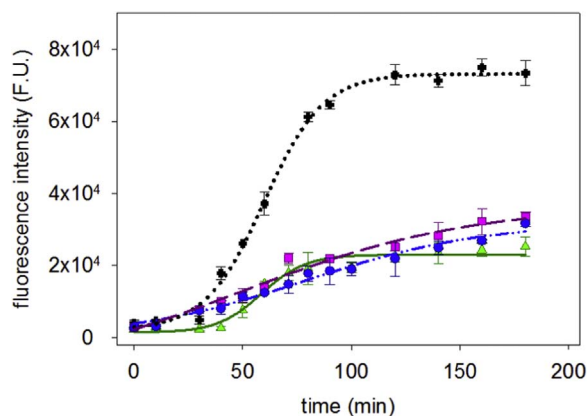


Fig. 4. Time dependence of insulin amyloid fibrillization monitored using ThT fluorescence. Insulin (10 μM) fibrillization in absence (crosses) and in presence of nanoparticles ($116 \mu\text{g}\cdot\text{ml}^{-1}$) NP-FeDEX_1 (triangles), NP-FeDEX_2 (squares) and NP-FeDEX_3 (circles) is shown. Each experiment was performed in triplicates, error bars represent the average deviation for repeated measurements of three separate samples.

The most significant shift in the nucleation lag time was observed for NP-FeDEX_1 (Fig. 4, triangles) possessing the smallest diameter. As a consequence the value determined for steady-state is lower (~70% decreasing) assuming reduction of insulin in form of amyloid fibrils. Interestingly, time-dependences of insulin fibrillization in presence of NP-FeDEX_2 (Fig. 4, squares) and NP-FeDEX_3 (Fig. 4, circles) have lag phases comparable to lag phase of insulin fibrillization and fluorescence intensities are slowly increasing with time. The steady-state values achieved about ~40% of the fluorescence value detected for untreated fibrillization. These data assume that inhibitory activities of studied nanoparticles can result from inhibition of nuclei formation and also from inhibition of fibril polymerization in elongation phase of growth curves.

There is a growing interest in studying the interaction of magnetite nanoparticles with amyloidogenic proteins. Maghemite ($\gamma\text{-Fe}_2\text{O}_3$) nanoparticles were found to bind to insulin fibrils without affecting the kinetics of the insulin fibrillization process [21,22]. We have previously shown that Fe_3O_4 -based nanoparticles are able to affect amyloid aggregation of lysozyme [12]. It was shown that physico-

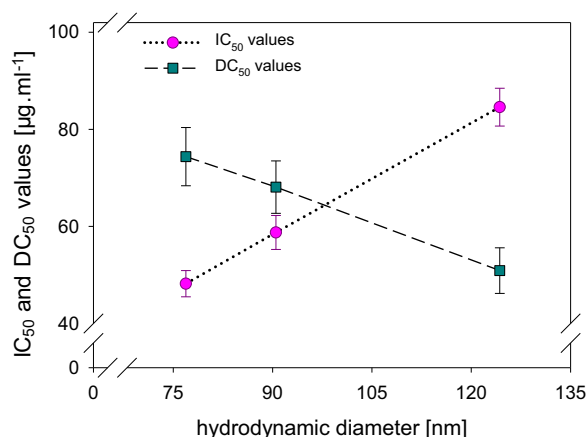


Fig. 5. Dependence of IC₅₀ (circles) and DC₅₀ values (squares) on the hydrodynamic diameter of NP-FeDEXs.

chemical properties of nanoparticles such as type of coating layer, charge, concentration, etc. affect their anti-amyloid activities [12,15,19]. The obtained results imply that nanoparticle concentration as well as nanoparticle physico-chemical properties, mainly hydrodynamic diameter influence the anti-amyloid activities of newly prepared iron-based nanoparticles coated with dextran. It is interesting that inhibiting activities characterized by IC₅₀ values have upward trend with increasing hydrodynamic diameter of NP-FeDEXs (Fig. 5, circles). The opposite downward trend is detected for DC₅₀ values (Fig. 5, squares). These findings suggest an important correlation between the size and anti-amyloid activities of studied NP-FeDEXs.

We suggest that smaller nanoparticles exhibiting higher surface/volume ratio provided higher ability for protein monomers to adsorb on their surface. This may lead to decrease of concentration of free protein in solution and thus block the formation of the amyloid aggregates. Our assumption is supported by results from kinetic fibrillization experiments and IC₅₀ values in low μg ml⁻¹ concentrations. Wu et al. [11] suggested that extent of protein structural changes is determined by protein concentration on the nanoparticle surface forming various crowded surface environments preferring protein–protein or protein–NP interactions. The effect of nanoparticle size and shape was observed also in the case of amyloid formation of Aβ peptide. O’Brien et al. [23] detected that smaller nanoparticles have the largest influence on the earliest amyloid oligomers of transthyretin. In

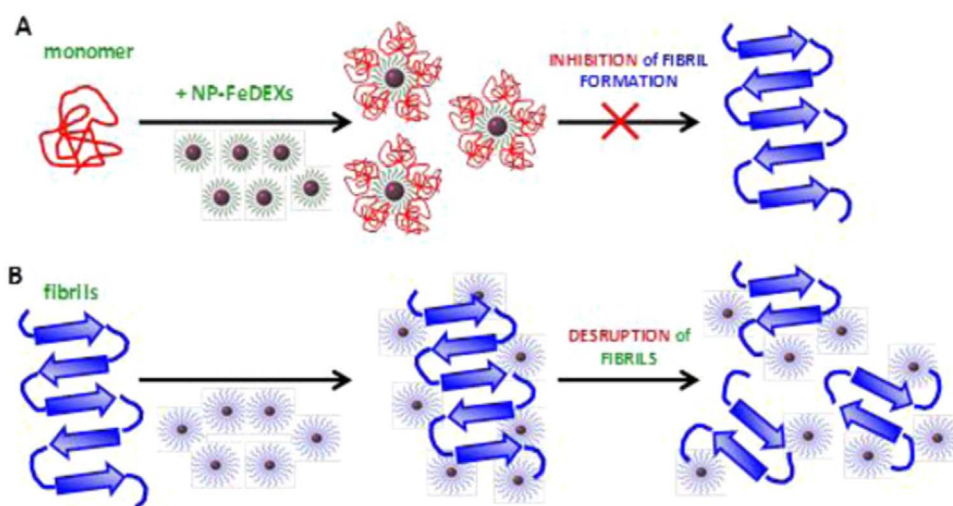
our previous work we have found that presence of the coating layer on the nanoparticles significantly affect their size and anti-amyloid properties [24].

The opposite dependence of NP-FeDEXs size on destruction of insulin amyloid fibrils could be explained by larger number of possible interactions between insulin fibrils and nanoparticles coated with dextran of the highest molecular mass. We hypothesize that this larger number of possible side-chain interactions of 70 kDa dextran-modified nanoparticles with beta-sheets in fibrils result into disruptions of interaction stabilized beta-sheets leading to disruption of fibrils. Both possible scenario of inhibition and destroying ability of dextran coated nanoparticles on insulin amyloid aggregation are presented in Scheme 1.

Similar effect of nanoparticles with different coating on amyloid aggregation of Aβ peptide was shown by Mahmoudi et al. [19]. Decreasing of the neutral (dextran coated NPs) and negative (carboxydextran coated NPs) nanoparticles size led to the increasing of the length of lag phase. The positively charged nanoparticles exhibit “dual” effect on the length of lag phase. They proposed that positive charge at the surface of SPIONs can induce conformational changes to the protein monomers which could result in a significant decrease in the lag time if the altered protein conformation is more prone to fibrillization.

4. Conclusions

The obtained results indicate that all three types of dextran coated magnetite nanoparticles have ability to interfere with insulin amyloid aggregation. Presence of NP-FeDEXs leads to the significant inhibition of insulin fibrillization and destruction of insulin amyloid fibrils. The extent of anti-amyloid activities depends on the properties of NP-FeDEXs, mainly on their size (hydrodynamic diameter) determined by the molecular mass of dextran molecules used for nanoparticle coating. The inhibiting ability determined by IC₅₀ values is positively related to the size of studied nanoparticles. The most effective inhibiting activity is exhibited by the smallest nanoparticles coated by 15–20 kDa dextran. On the contrary, destroying activity determined by DC₅₀ values decreased with increasing size of nanoparticles. The highest destroying activity was observed for the biggest NP-FeDEX coated with 70 kDa dextran. Our results imply that different molecular weight of dextran used for nanoparticles coating influence their size (hydrodynamic diameter) and anti-amyloid activities. The obtained results also indicate that major role in anti-amyloid activities of studied nanopar-



Scheme 1. Scheme illustration of possible scenario of inhibition (A) and destroying (B) ability of dextran coated nanoparticles on insulin amyloid aggregation. Presence of NP-FeDEXs leads to the significant inhibition of insulin fibrillization (scenario A) due to adsorption of protein monomers on the nanoparticle surfaces resulting in the decrease of free protein molecules in solution and thus inhibit the formation of amyloid aggregates. Disruption of the insulin amyloid fibrils (scenario B) is result of the large number of side-chain interactions of NP-FeDEXs with fibrillar beta-sheets, the main structural motif of amyloid fibrils, leading to their depolymerization.

titles is played by magnetite core as dextran itself has no ability to affect insulin amyloid aggregation. We assume that the presented findings represent a starting point for the application of the most active NP-FeDEXs as therapeutic agents targeting insulin-associating amyloidosis.

Author contributions

The manuscript was written through contributions of all authors. All authors have given approval to the final version of the manuscript.

Acknowledgment

This work was supported by the research grant projects 26220220005, 26110230097 and 26110230061 in frame of SF EU, VEGA 0181 and LD13021 and LO1305 (Ministry of Education, Czech Republic).

References

- [1] J. Hardy, D.J. Selkoe, The amyloid hypothesis of Alzheimer's disease: progress and problems on the road to therapeutics, *Science* 297 (5580) (2002) 353–356.
- [2] F. Chiti, C.M. Dobson, Protein misfolding, functional amyloid, and human disease, *Annu. Rev. Biochem.* 75 (2006) 333–366.
- [3] C.M. Dobson, Protein folding and misfolding, *Nature* 426 (2003) 884–890.
- [4] M. Sunde, C. Blake, The structure of amyloid fibrils by electron microscopy and X-ray diffraction, *Adv. Protein Chem.* 50 (1997) 123–159.
- [5] D.B. Teplow, Structural and kinetic features of amyloid beta-protein fibrillogenesis, *Amyloid* 5 (1998) 121–142.
- [6] F.E. Dische, C. Wernstedt, G.T. Westermark, P. Westermark, M.B. Pepys, J.A. Rennie, J.S.G. Gilbey, P.J. Watkins, Insulin as an amyloid-fibril protein at sites of repeated insulin injections in a diabetic patient, *Diabetologia* 31 (1988) 158–161.
- [7] F.G. De Felice, S.T. Ferreira, Beta-amyloid production, aggregation, and clearance as targets for therapy in Alzheimer's disease, *Cell Mol. Neurobiol.* 22 (2002) 545–563.
- [8] I. Khlistunova, J. Biernat, Z.P. Wang, M. Pickhardt, M. von Bergen, Z. Gazova, E. Mandelkow, E.-M. Mandelkow, Inducible expression of Tau repeat domain in cell models of tauopathy. Aggregation is toxic to cells but can be reversed by inhibitor drugs, *J. Biol. Chem.* 281 (2006) 1205–1214.
- [9] S. Rocha, A.F. Thünemann, C. Pereira, M. Coelho, H. Möhwald, G. Brezesinski, Influence of fluorinated and hydrogenated nanoparticles on the structure and fibrillogenesis of amyloid beta-peptide, *Biophys. Chem.* 137 (2008) 35–42.
- [10] H. Skaat, G. Shafir, S. Margel, Acceleration and inhibition of amyloid- β fibril formation by peptide-conjugated fluorescent-maghemite nanoparticles, *J. Nanopart. Res.* 13 (2011) 3521–3534.
- [11] W.H. Wu, X. Sun, Y. Yu, J. Hu, L. Zhao, Q. Liu, Y. Zhao, Y. Li, TiO₂ nanoparticles promote beta-amyloid fibrillation in vitro, *Biochem. Biophys. Res. Commun.* 373 (2008) 315–318.
- [12] A. Bellova, E. Bystrenova, M. Koneracka, P. Kopcansky, F. Valle, N. Tomasovicova, M. Timko, J. Bagelova, F. Biscarini, Z. Gazova, Effect of Fe₃O₄ magnetic nanoparticles on lysozyme amyloid aggregation, *Nanotechnology* 21 (2010) 065103.
- [13] S. Linse, C. Cabaleiro-Lago, W.-F. Xue, I. Lynch, S. Lindman, E. Thulin, S.E. Radford, K.A. Dawson, Nucleation of protein fibrillation by nanoparticles, *Proc. Natl. Acad. Sci. USA* 104 (2007) 8691–8696.
- [14] A.M. Saraiva, I. Cardoso, M.J. Saraiva, K. Tauer, M.C. Pereira, M.A.N. Coelho, H. Möhwald, G. Brezesinski, Randomization of amyloid- β -peptide(1–42) conformation by sulfonated and sulfated nanoparticles reduces aggregation and cytotoxicity, *Macromol. Biosci.* (10) (2010) 1152–1163.
- [15] K. Siposova, M. Kubovcikova, Z. Bednarikova, M. Koneracka, V. Zavisova, A. Antosova, P. Kopcansky, Z. Daxnerova, Z. Gazova, Depolymerization of insulin amyloid fibrils by albumin-modified magnetic fluid, *Nanotechnology* 23 (2010) 055101.
- [16] L. Xiao, D. Zhao, W.-H. Chan, M.M.F. Choi, H.-W. Li, Inhibition of beta 1–40 amyloid fibrillation with N-acetyl-L-cysteine capped quantum dots, *Biomaterials* 31 (2010) 91–98.
- [17] M. Zhang, Y. Yu, Ch-X. Wang, Y.-L. Yang, Ch Wang, Nanomaterials for reducing amyloid cytotoxicity, *Adv. Mater.* 25 (28) (2013) 3780–3801.
- [18] N. Sounderya, Y. Zhang, Use of core/shell structured nanoparticles for biomedical applications, *Recent Pat. Biomed. Eng.* 1 (2008) 34–42.
- [19] M. Mahmoudi, F. Quinlan-Pluck, M.P. Monopoli, S. Sheibani, H. Vali, K.A. Dawson, I. Lynch, Influence of the physicochemical properties of superparamagnetic iron oxide nanoparticles on amyloid β protein fibrillation in solution, *ACS Chem. Neurosci.* 20 (2013) 475–485.
- [20] R.S. Molday, D. Mackenzie, Immunospecific ferromagnetic iron-dextran reagents for the labeling and magnetic separation of cells, *J. Immunol. Methods* 52 (3) (1982) 353–367.
- [21] H. Skaat, M. Sorci, G. Belfort, S. Margel, Effect of maghemite nanoparticles on insulin amyloid fibril formation: selective labeling, kinetics, and fibril removal by a magnetic field, *J. Biomed. Mater. Res. A* 91 (2009) 342–351.
- [22] A. Skaat, G. Belfort, S. Margel, Synthesis and characterization of fluorinated magnetic core-shell nanoparticles for inhibition of insulin amyloid fibril formation, *Nanotechnology* 20 (2009) 225106.
- [23] E.P. O'Brien, J. Straub, B.R. Brooks, D. Thirumalai, Influence of nanoparticle size and shape on oligomer formation of an amyloidogenic peptide, *J. Phys. Chem. Lett.* 2 (2011) 1171–1177.
- [24] K. Siposova, E. Bystrenova, A. Antosova, M. Koneracka, V. Zavisova, P. Kopcansky, Z. Gazova, Attenuation of the insulin amyloid aggregation in presence of Fe₃O₄-based magnetic fluids, *Gen. Physiol. Biophys.* 32 (2013) 209–214.